NUMERICAL AND EXPERIMENTAL ANALYSIS OF AXI-SYMMETRIC FLOWS OF VISCOPLASTIC LIQUIDS THROUGH AN EXPANSION FOLLOWED BY A CONTRACTION

Mônica F. Naccache
Pontifícia Universidade Católica do Rio de Janeiro, RJ 22453-900, Brazil
naccache@mec.puc-rio.br

Luiz F. Sauerbronn
Pontifícia Universidade Católica do Rio de Janeiro, RJ 22453-900, Brazil
lfsauer@olimpo.com.br

P. R. Varges
Pontifícia Universidade Católica do Rio de Janeiro, RJ 22453-900, Brazil
pri_varges@yahoo.com.br

Paulo R. Souza Mendes
Pontifícia Universidade Católica do Rio de Janeiro, RJ 22453-900, Brazil
pmendes@mec.puc-rio.br

Abstract. *The internal flow of viscoplastic liquids through an abrupt axissymmetric expansion followed by an abrupt contraction is studied. This situation is representative of numerous flows found in industrial processes, such as extrusion, mold filling and liquid displacement in porous media. The yield stress strongly affects the flow pattern as well as the pressure drop along the channel. In this work, numerical solutions were obtained by solving the conservation equations of mass and momentum via the finite volume method. The Generalized Newtonian Liquid constitutive equation was employed, in conjunction with a recently proposed viscosity function to model the viscoplastic behavior of the liquid. The numerical results were obtained for steady, inertialess flow. Flow visualization experiments were also conducted. The liquids employed were Carbopol aqueous solutions at different concentrations containing micron-size spheres to promote light reflection. The test section was built in transparent plexiglas. A metering pump was employed to move the liquid in open loop. A laser sheet was employed to illuminate a plane containing the channel axis, and a CCD camera recorded the particle paths. Yielded and unyielded regions are observed, as well as an apparent discontinuity of the velocity field. The viscoplastic liquid seems to "fracture" near the core region of the flow, and an unyielded region appears in the large-diameter portion of the channel, away from the symmetry line.*

Keywords: *Viscoplastic liquid, contraction/expansion flows (up to 5 keywords)*

1. Introduction

Flow of liquids through ducts with expansions and contractions are found in several industrial processes, such as extrusion, mold filling and liquid displacement through porous media. In many cases, the fluid used has a viscoplastic behavior. Viscoplastic materials have a purely viscous non-Newtonian behavior, and their main characteristic is the presence of a yield stress. Above the yield stress the material behaves as a liquid, and, below it, as a solid. However, it is worth mentioning that there are several recent studies in the literature that discuss the existence of the yield stress.

Barnes (1999a, 1999b) performed a comprehensive review about yield stress materials, reviving the argument that yield stress actually does not exist. He shows, for a large number of materials typically classified as viscoplastics, that when careful measurements are performed below the "yield stress," it is found that flow actually takes place. Then, the viscosity function looks like a bi-viscosity model, with very high viscosity at small shear rates and lower viscosities for larger shear rates. However, it is suggested that an apparent yield stress can exist as a useful mathematical description of limited data, over a given range of flow conditions.

Alexandrou *et al.* (2001) studied numerically the flow of Herschel-Bulkley fluids in a three-dimensional expansion. The ducts have square cross sections, and the results were obtained for a 2:1 and a 4:1 expansion rate. The effects of Reynolds number and Bingham number on flow pattern and pressure distribution were investigated. It was observed that a strong interplay between the Reynolds and Bingham numbers occurs, and they influence the formation and break up of stagnant zones in the corner of the expansion. Souza Mendes *et al.* (2000) performed an experimental and numerical analysis of the flow of viscoplastic fluids through a converging-diverging channel. They observed experimentally a flow pattern transition, for a critical value of the ratio between the length and the diameter of the central region, indicating a possible material fracture. However, the viscosity model used in the numerical simulation was not capable to predict this

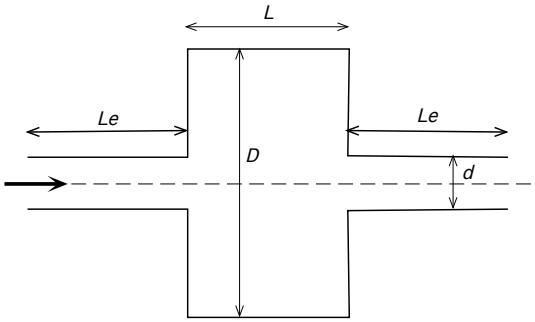

Figure 1. The geometry.

behavior. In a more recent work (Reis and Naccache, 2003) performed a more detailed analysis of the flow in this same geometry using the Carreau model for the viscosity function. Despite the results show large velocities variations in the large-diameter duct, the results are still not conclusive about a possilble material fracture.

The flow of Bingham materials through a 1×2 abrupt expansion was analyzed numerically by Vradis and Ötügen (1997). They observed that the reattachment length increases with the Reynolds number, decreases with yield stress and is essentially independent of the expansion ratio. An experimental study of the flow through axisymmetric expansions was performed by Pak *et al.* (1990). This work analyzes the influence of Reynolds number on separation zones and reattachment length of Newtonian, purely viscous non-Newtonian, and viscoelastic fluids in abrupt axisymmetric expansions. It was observed that the reattachment length for purely viscous non-Newtonian fluids is almost the same as for Newtonian fluids. For laminar flows, elasticity decreases the reattachment length, while for turbulent flows the opposite trend is observed.

In this work, the flow of non-Newtonian fluids through an abrupt axisymmetric expansion followed by an abrupt contraction is analyzed experimentally and numerically, using a recently proposed viscosity function (Souza Mendes and Dutra, 2004). The influence of yield stress on flow pattern is investigated and a comparison between numerical and experimental results is also performed.

2. Mathematical Modeling

The geometry analyzed is shown in Fig. 1. The flow is laminar, steady and axisymmetric. All the properties are considered to be constant and viscous dissipation is negligible. The mechanical behavior of the non-Newtonian fluid is modeled by the Generalized Newtonian Liquid constitutive equation (GNL) (Bird *et al.*, 1987):

$$\boldsymbol{\tau} = \eta(\dot{\gamma})\dot{\boldsymbol{\gamma}} \tag{1}$$

where $\boldsymbol{\tau}$ is the extra-stress tensor, $\dot{\boldsymbol{\gamma}}$ is the rate-of-deformation tensor, defined as $\mathrm{grad}\,\mathbf{v} + (\mathrm{grad}\,\mathbf{v})^{\mathrm{T}}$, $\mathbf{v}$ is the velocity vector and η is the viscosity function, given by a recently proposed model (Souza Mendes and Dutra, 2004). The function proposed is continuous and presents a low shear-rate viscosity plateau, followed by a sharp viscosity drop at a threshold shear stress value (yield stress), and a subsequent power-law region. The equation is given bellow:

$$\eta = \left(1 - \exp\left(-\eta_0\dot{\gamma}/\tau_0\right)\right)\left(\frac{\tau_0}{\dot{\gamma}} + K\dot{\gamma}^{n-1}\right) \tag{2}$$

The physical meaning of the parameters can be understood with the aid of Fig.2. η_0 is equal to the ratio $\tau/\dot{\gamma}$ provided τ is smaller enough than τ_0 to ensure that $\dot{\gamma}$ is within the zero-shear rate plateau region. The yield stress is the value of the stress modulus at the plateau region. The behavior index n is the slope of the power-law region. The intercept of the extrapolated power-law region straight line with the vertical line at $\dot{\gamma} = 1\ \mathrm{s}^{-1}$ occurs at $\tau = K$.

The mass and momentum conservation equations for an incompressible fluid, and using the Generalized Newtonian Fluid constitutive equation, are given by:

$$\mathrm{div}\mathbf{v} = 0 \tag{3}$$

$$\rho\mathrm{grad}\mathbf{v}\cdot\mathbf{v} = -\mathrm{grad}p + \mathrm{div}(\eta\mathrm{grad}\mathbf{v}) \tag{4}$$

where $\mathbf{v} = u\mathbf{i} + v\mathbf{j}$ is the velocity vector, u is the axial velocity component, v is the radial velocity component, p is the pressure, ρ is the fluid density, and η is the viscosity function, given by eq.(2). Using cylindrical coordinates, the governing equations are given bellow.

Mass conservation equation:

$$\frac{1}{r}\frac{\partial}{\partial r}\left(rv\right) + \frac{\partial}{\partial x}\left(u\right) = 0 \tag{5}$$

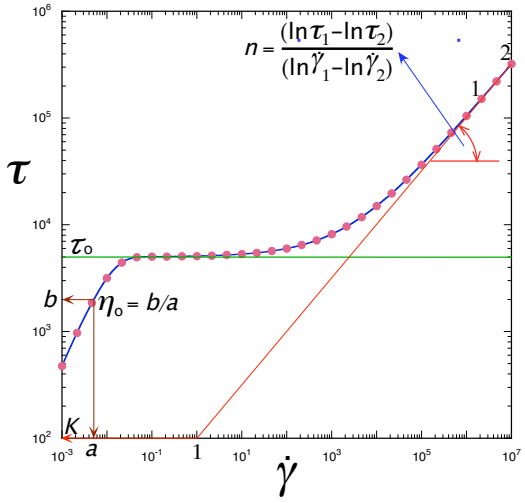

Figure 2. The viscosity function.

Axial momentum conservation equation:

$$\frac{1}{r}\frac{\partial}{\partial r}\left(\rho r v u\right)+\frac{\partial}{\partial x}\left(\rho u u\right)=\frac{1}{r}\frac{\partial}{\partial r}\left(\eta r\frac{\partial u}{\partial r}\right)+\frac{\partial}{\partial x}\left(\eta\frac{\partial u}{\partial x}\right)+\frac{1}{r}\frac{\partial}{\partial r}\left(\eta r\frac{\partial v}{\partial x}\right)+\frac{\partial}{\partial x}\left(\eta\frac{\partial u}{\partial r}\right)-\frac{\partial p}{\partial x} \tag{6}$$

Radial momentum conservation equation:

$$\frac{1}{r}\frac{\partial}{\partial r}\left(\rho r v v\right)+\frac{\partial}{\partial x}\left(\rho v u\right)=\frac{1}{r}\frac{\partial}{\partial r}\left(\eta r\frac{\partial v}{\partial r}\right)+\frac{\partial}{\partial x}\left(\eta\frac{\partial v}{\partial x}\right)+\frac{1}{r}\frac{\partial}{\partial r}\left(\eta r\frac{\partial v}{\partial r}\right)+\frac{\partial}{\partial x}\left(\eta\frac{\partial u}{\partial r}\right)-2\eta\frac{v}{r^2}-\frac{\partial p}{\partial r} \tag{7}$$

where x and r are the axial and radial coordinates, respectively.

The boundary conditions are the usual no-slip and impermeability conditions at solid boundaries ($u = v = 0$), symmetry condition at centerline ($\partial u/\partial r = 0$ and $v = 0$), and developed flow at outlet ($\partial/\partial x = 0$). At the inlet, axial velocity is considered uniform ($u = u_{mean}$ and $v = 0$). The length of upstream and downstream tubes was chosen to guarantee flow development before the entrance of the large-diameter duct, and the exit of the downstream tube ($L_i = 20R_i$).

3. Numerical Solution

The conservation equations of mass and momentum are discretized by the finite volume method described by Patankar (1980). Staggered velocity components are employed to avoid unrealistic pressure fields. The SIMPLE algorithm (Patankar, 1980) is used, in order to couple the pressure and velocity. The resulting algebraic system is solved by the TDMA line-by-line algorithm (Patankar, 1980) with the block correction algorithm (Settari and Aziz, 1973) to increase the convergence rate.

To define the computational mesh, the domain was divided in five zones. Two zones correspond to the entrance and exit ducts. The other three zones were defined in the central duct: one corresponds to the core region, until a radius equal to the entrance duct radius (i.e., from $r = 0$ to $r = d/2$); the second one goes from $r = d/2$ to $r = (D - d)/4$; and the last one goes from $r = (D - d)/4$to $r = D/2$. The mesh employed was uniform in the axial and radial directions in each zone, with a more refined mesh in the central tube. To validate the numerical solution, extensive grid tests were performed. The error obtained for the product of the friction factor and the Reynolds number ($fRe = 8\dot{\gamma}_c D/\bar{u}$) with respect to the exact value, for a fully developed Newtonian flow at the downstream tube with the mesh used (202x230), was equal to 4%. For the non-Newtonian fluids, a comparison of velocity profiles obtained with six different meshes at radial direction was performed, showing a very small difference (less than 1%) between the mesh used and more refined meshes.

4. Experimental Visualization

Figures 3-4 show the scheme and a photo of the test section, where flow visualization were conducted. The test section was built in transparent plexiglas, and a metering pump was employed to move the liquid in open loop. A laser sheet was employed to illuminate a plane containing the channel axis. A CCD camera recorded the particle paths. A wide range of length-to-diameter and small diameter to large diameter ratios could be used in the test section, just changing the central duct region of the test section. The liquids employed in the visualizations were Carbopol aqueous solutions containing micron-size spheres to promote light reflection.

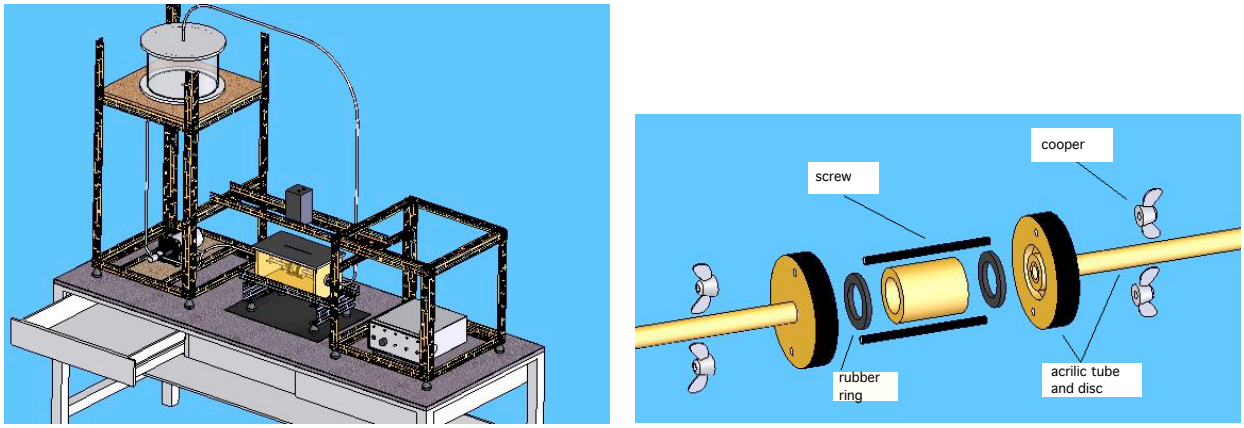

Figure 3. Scheme of the experimental apparatus and the test section.

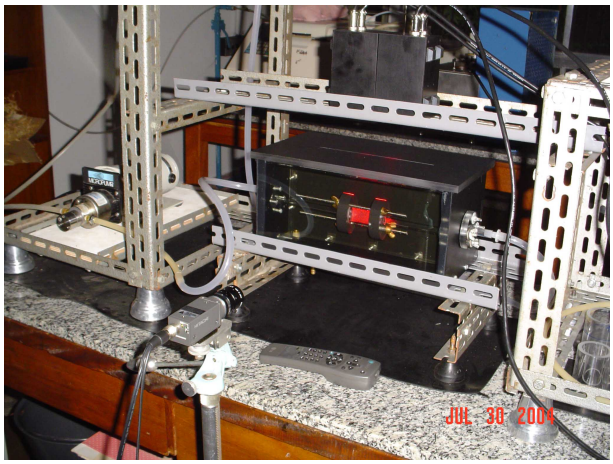

Figure 4. Overall view of the experimental apparatus.

5. Results and Discussion

The numerical results were obtained for a fixed geometry. The ratio between the central and the entrance ducts diameters was equal to 4.88, and the ratio between the length and the diameter of the central duct was equal to 0.5. This geometry was chosen based on the results previously obtained in Souza Mendes et al. (2000), where it was observed that a material fracture could occur at this range of geometrical parameters. The fluid used in the experimental visualization was the Carbopol aqueous solution with a weight concentration of 15%, and the rheological parameters are: $\eta_0 = 6000$ Pa.s, $\tau_0 = 1.5$ Pa.s, $K = 2.53$ Pa.s^{-n} and $n = 0.5$. The influence of the dimensionless yield stress number, the yield number, on flow pattern are now presented and analyzed. The yield number is defined by $\tau_0' \equiv \tau_0/\tau_w$, where τ_w is the shear stress in the developed flow region of the entrance duct wall. All the results were obtained for low Reynolds numbers. The Reynolds number is defined as $Re = \rho\bar{v}d/\eta_w$, where $\eta_w = \eta(\dot{\gamma}_w)$ is the viscosity evaluated in the developed flow region of the entrance duct wall.

Figure 5 shows the axial velocity contour for a low yield number, $\tau_0' = 0.05$. It shows that the fluid flows through all the central duct, with very low velocities ($u < 10^{-4}$) detected near the central duct wall. The dimensionless stress field (τ') for the same case can be analyzed in Fig 6. It is worth mentioning that according to the viscosity function used in the numerical simulations, bellow the yield stress limit (i.e., $\tau' < 1$), the fluid behaves as a Newtonian fluid with a very large viscosity, and therefore, flow occurs with very low strain rates. This region is called the unyielded region. It can be noted that only in a very small region near the wall the stress is bellow the yield stress limit, which is in agreement with the velocity field results. As the yield number is increased to values equal to 0.14 (Fig. 7) and 0.6 (Fig. 8), it can be observed that the unyielded region (the blue zone) increases. The limit between the yielded and the unyielded regions characterizes the so-called material fracture. Also, it can be noted a small unyielded region near the centerline for the larger yield stress fluids. In this region, the stress is also lower than yield stress, and therefore the viscosity is extremely high. This region is called the plug-flow region, where there is flow, but the strain rates are too small so that the velocity profile is almost constant.

Figure 9 show the viscosity function for $\tau_0' = 0.6$. It can be noted that in the unyielded regions, viscosity values are very high, as expected.

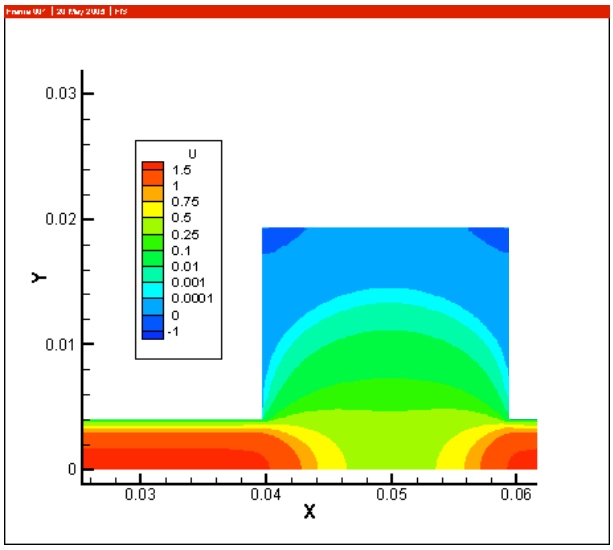

Figure 5. Streamlines for $\tau_0' = 0.05$.

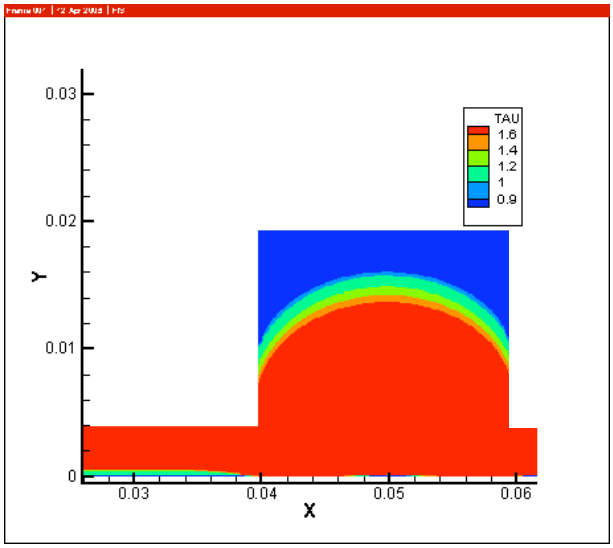

Figure 6. Dimensionless stress field for $\tau_0' = 0.05$.

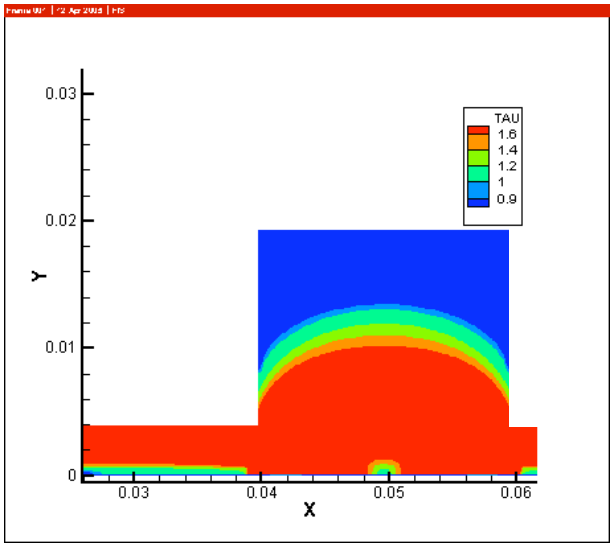

Figure 7. Dimensionless stress field for $\tau_0' = 0.14$.

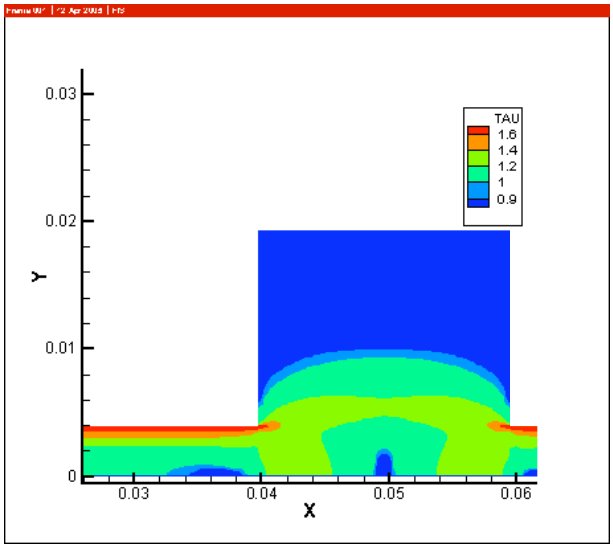

Figure 8. Dimensionless stress field for $\tau_0' = 0.6$.

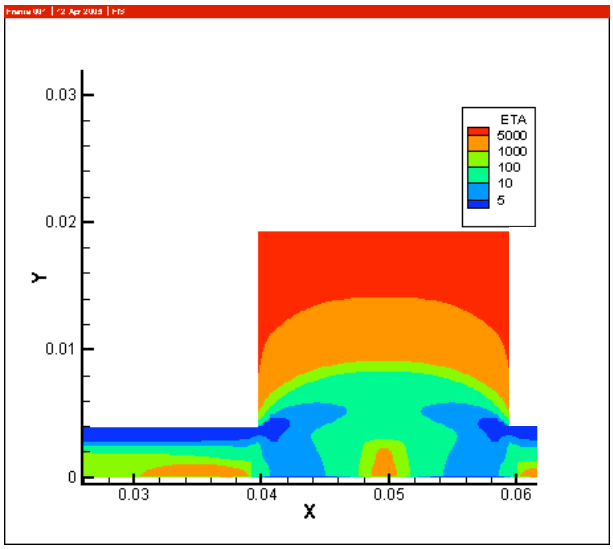

Figure 9. Viscosity field for $\tau_0' = 0.6$.

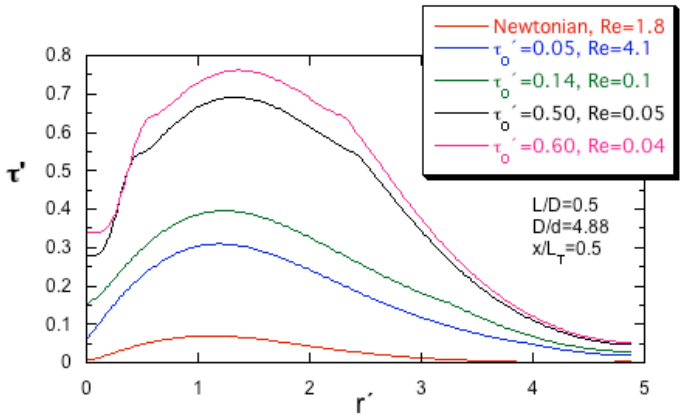

Figure 10. Dimensionless stress tensor modulus at $x/L_T = 0.5$ for Newtonian and visplastic fluids with $\tau_0' = 0.05, 0.14, 0.50$ and 0.60.

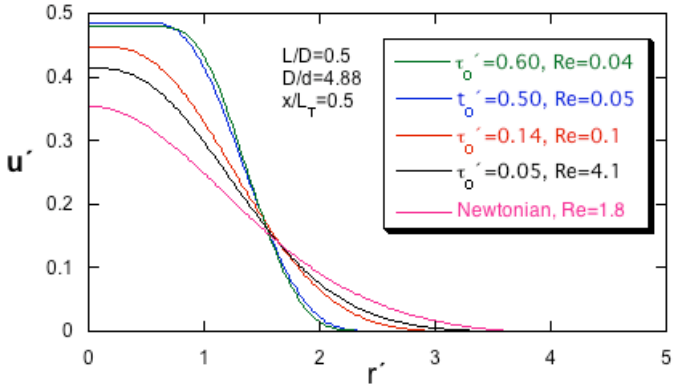

Figure 11. Velocity profile at $x/L_T = 0.5$ for Newtonian and viscoplastic fluids with $\tau_0' = 0.05, 0.14, 0.50$ and 0.60.

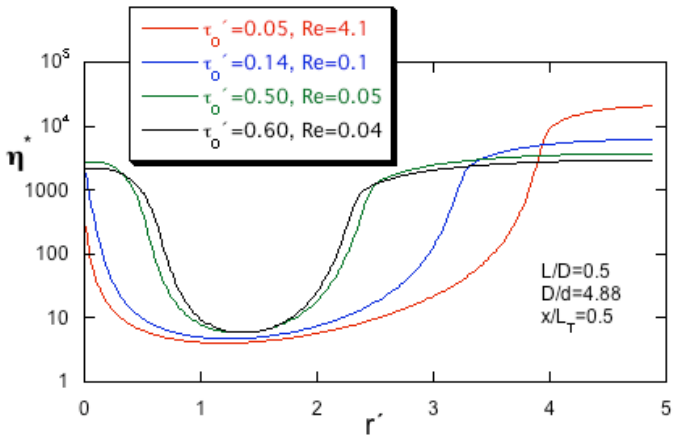

Figure 12. Dimensionless viscosity at $x/L_T = 0.5$ for visplastic fluids with $\tau_0' = 0.05, 0.14, 0.50$ and 0.60.

Figure 10 shows the dimensionless modulus of stress tensor ($\tau' = \tau/\tau_w$, $\tau \equiv \sqrt{1/2\mathrm{tr}\boldsymbol{\tau}^2}$) in the center of the central duct ($x/L_T = 0.5$), for Newtonian and viscoplastic fluids. For Newtonian fluid and viscoplastic fluids with lower yield stress, the stress varies amost linearly for low radius, reaching a maximum at $r' = 1$, when it starts to decrease. This point is shifted to higher r' values as the yield stress increases. Figures 11 and 12 show the velocity, and dimensionless viscosity profiles in the same position ($x/L_T = 0.5$). The dimensionless viscosity is defined as $\eta' \equiv \eta/\eta_w$. It can be observed that for higher yield numbers the velocity drop is more abrupt, going to almost zero at lower values of the radius. The unyielded regions can be better identified analyzing these graphics. The plug flow region, near the core, is the region of lower stresses, extremely high viscosities, and almost constant velocity. The plug flow region ends when the slope of the curve of the modulus of stress tensor changes. Then, the velocity starts to decrease, increasing the strain rates, leading to a viscosity decay. When the velocity variations become smoother, the strain rates decrease, and the viscosity increases. When the stress reaches the yield stress limit, near the central duct wall ($r' > 1$), another unyielded zone appears, but now the velocity values are almost zero, due to the boundary condition at wall. The material "fracture" occurs at the point where the dimensionless stress modulus reaches the dimensionless yield stress. It can be observed that this point is the same one where velocity reaches "zero" (or a very low value), or where viscosity reaches an almost constant plateau with extremely high value.

Table 1. Position of material fracture at *x=Le+L/2*

τ_0'	r'_{exp}	r'_{num}
0.05	3.6	3.7
0.14	2.3	3.3

Finally, Fig. 13 shows the experimental flow visualization for $\tau_0' = 0.05$ and 0.14. It can be observed a large particle concentration in the central duct, in a line inside the central duct, where the flow velocity tends to zero and the material fracture occurs. The numerical results for the flow pattern are in reasonable agreement with the results of the visualization experiments. However, a lack of symmetry is observed experimentally, probably due to fluid elasticity, which is not considered in the numerical solution. The position of the material fracture at the center of the central duct (*x=Le+L/2*) was compared with the ones obtained with the numerical solution for these two cases ($\tau_0' = 0.05$ and 0.14), and are presented in Table 1. It can be observed that the agreement is better for the lower yield stress.

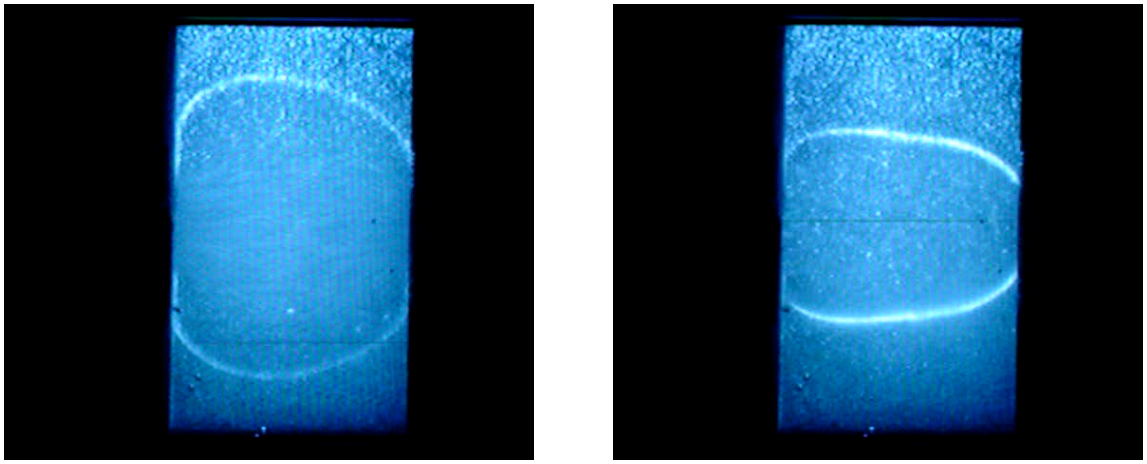

Figure 13. Experimental flow visualization, for $\tau_0' = 0.05$ and 0.14.

6. Concluding Remarks

In this work a numerical and experimental study of the flow of viscoplastic liquids through an abrupt axissymmetric expansion followed by an abrupt contraction was performed. The numerical solution was obtained by solving the governing equations via the finite volume method. The viscoplastic behavior was modeled by the Generalized Newtonian Liquid constitutive equation, with the viscosity function proposed by Souza Mendes and Dutra. Flow visualization experiments were also conducted. The results obtained show two distinct zones in the central duct. An yielded region, near the core, and an unyielded region near the wall. Between these regions, a material fracture seems to occur. The comparison between numerical and experimental results were in good agreement, but the experimental results showed a lack of symmetry, probably due to fluid elasticity, which is not considered in the numerical modeling.

7. Acknowledgements

Financial support for the present research is provided by CNPq and MCT.

8. References

Alexandrou, A. N., McGilvreay, T. M. and Burgos, G., 2001, "Steady Herschel-Bulkley fluid flow in three-dimensional expansions", J. Non-Newtonian Fluid Mech., Vol. 100, pp.77–96.

Barnes, H. A., 1999a, "A brief history of the yield stress", Appl. Rheology, Vol. 9, No. 6, pp. 262–266.

Barnes, H. A., 1999b, "Yield stress–a review, or $\pi\alpha\nu\tau\alpha\rho\epsilon$–everything flows?", J. N N Fluid Mech., Vol. 81, pp. 133–178.

Bird, R.B., Armstrong, R.C. and Hassager, O., 1987, Dynamics of Polymeric Liquids, Wiley.

Naccache, M.F. and Souza Mendes, P.R., 1997, "Abrupt Expansion Flows of Bingham Materials", Proc. of XIV Brazilian Congress of Mechanical Engineering, in CDROM.

Pak, B., Cho, Y. I. and Choi, S. U. S., 1990, "Separation and Reattachment of Non-Newtonian Fluid Flows in a Sudden Expansion Pipe", J. Non-Newt. Fluid Mech., Vol. 37, pp.175–199.

S. V. Patankar, 1980. Numerical Heat Transfer and Fluid Flow (Hemisphere Publishing Corporation).

Reis Jr., L. A., 2003, "Flow of viscoplastic materials through an abrupt expansion and contraction", Masters Thesis, Department of Mechanical Engineering, Catholic University of Rio de Janeiro. (in portuguese)

Reis Jr., L. A., Naccache, M.F., 2003, “Analysis of non-Newtonian flows through contractions and expansions”, Proc. of XVII Brazilian Congress of Mechanical Engineering, in CDROM.

Settari, S. and Aziz, K., 1973., "A Generalization of the Additive Correction Methods for the Iterative Solution of Matrix Equations", SIAM J. Num. Anal., Vol. 10, pp.506–521.

Souza Mendes, P. R., Naccache, M. F. and Vinagre, H. T. M., 2000, "On numerical simulations of complex flows of viscoplastic materials", Proc. ASME-IMECE, FED-Vol. 252, pp. 17–23.

Souza Mendes, P.R., Dutra, E.S.S., 2004, ”Viscosity function for yield-stress liquids”, Appl. Rheol., Vol. 14, pp. 296-302.

Vradis, G. C., Ötügen, M. V., 1997, ”The Axisymmetric Sudden Expansion Flow of a Non-Newtonian Viscoplastic Fluid”, J. of Fluids Engineering, Vol. 110, pp.193–200.

9. Responsibility notice

The authors are the only responsible for the printed material included in this paper